Electronic Supplementary Material (ESI) for Journal of Materials Chemistry C.

Supporting Information

Efficient Triphenylamine-based Polymorphs with Different Mechanochromism and Lasing Emission: Effects of Molecular Packing and Intermolecular Interactions

Bing Fang,[a] Manman Chu,[b] Zhen Wu,[a] Yan Shi,*[a] Yong Sheng Zhao,*[b] and Meizhen Yin*[a]
[a]State Key Laboratory of Chemical Resource Engineering, Beijing Advanced Innovation Center for Soft Matter Science and Engineering, BAIC-SM, Beijing Laboratory of Biomedical Materials, Beijing University of Chemical Technology, Beijing 100029, PR China.
[b]Key Laboratory of Photochemistry, Institute of Chemistry, Chinese Academy of Sciences, Beijing 100190, China.

Experimental Section

Materials and instruments. 4-bromo-N,N-diphenylaniline, (4-formylphenyl) boronic acid, potassium carbonate, 2-amino-5-methoxybenzenethiol, are purchased from Alfa Aesar Co. and use without further purification. The solvents for synthesis are common commercial grade. ^{1}H-NMR spectra are recorded on a Bruker 400 (400 MHz) spectrometer. Fluorescence spectroscopic studies are performed on a fluorescence spectrophotometer (Horiba Jobin Yvon FluoroMax-4 NIR, NJ, USA). UV–vis spectra are obtained on a spectrometer (Cintra 20, GBC, Australia). The percentage distribution of each lifetime component to the total decay curve and photoluminescence quantum yield is recorded using an Edinburgh Instruments FLS 980 fluorospectrophotometer. Powder X-ray diffraction (PXRD) patterns carried by a D/max2500 VB2+/PC X-ray diffractometer (Rigaku) using Cu Kα radiation in the 2θ range 5-40°. Scanning Electron Microscope: SEM observation was recorded on HITACHI S-4700 (Japan) SEM at an accelerating voltage of 10 kV. Samples (1 mg /mL^{-1}, T = 298.15 K) were vacuum sputtered with Pt to increase the contrast before SEM observation. TEM images were obtained by an H-800 (Hitachi) transmission electron microscope at an accelerating voltage of 200 kV. Our DFT calculations method were carried out using the Gaussion 09 program. Becke's three-parameter hybrid method using the Lee–Yang–Parr correlation functional (denoted as B3LYP) was employed and the 6-31G (d) basis set was used.

Synthesis of TPA-CHO

Under nitrogen atmosphere, 4-bromo-N,N-diphenylaniline (972 mg), (4-formylphenyl) boronic acid (540 mg), $Pd(PPh_3)_4$ (10 mg), potassium carbonate (500 mg) were suspend in the mixture water: ethanol: toluene = 1:2:10. The mixture was allowed to reflux at 80^{o}C for 12 h and then cooled to room temperature. After removing the solvent, the residue was dissolved in dichloromethane and then washed with water. The organic phase was dried over anhydrous Na_2SO_4. The obtained crude product used column chromatography to provide a yellow powder (yield 82%). ^{1}H NMR (400 MHz, DMSO) δ 10.03 (s, 1H), 7.96 (d, J = 8.3 Hz, 2H), 7.88 (d, J = 8.3 Hz, 2H), 7.71 (d, J = 8.7 Hz, 2H), 7.35 (d, J = 8.1 Hz, 4H), 7.09 (t, J = 11.7 Hz, 8H).

Synthesis of TZ-1, TZ-2 and **TZ-3**.

TZ-1: TPA-CHO (350 mg), 2-amino-5-methoxybenzenethiol (150 mg) was suspend into DMSO and was heated at 170°C for 12h. Then, the mixture was cooled to room temperature, poured into 200 mL ice-cold water, and extracted with dichloromethane for three times. The dichloromethane solution was washed with water and dried over anhydrous Na_2SO_4. The solvent was evaporated under vacuum. The resulting crude product was purified by column chromatography with n-hexane/CH_2Cl_2 (2:1, v/v) as eluent to afford pale yellow powder in a yield of 85% (Figure S1). The compound was characterized by ^{1}H-NMR and X-ray single crystal structural analysis. The detailed synthesis routine is provided in Scheme 1. ^{1}H NMR (400 MHz, DMSO) δ 8.11 (d, J = 8.5 Hz, 2H), 7.97 (d, J = 8.9 Hz, 1H), 7.85 (d, J = 8.5 Hz, 2H), 7.73 (dd, J = 13.3, 5.6 Hz, 3H), 7.36 (t, J = 7.9 Hz, 4H), 7.21-7.04 (m, 9H), 3.88 (s, 3H). ^{13}C NMR (101 MHz, CDCl3) δ 165.40 (s), 157.80 (s), 148.66 (s), 147.53 (s), 136.35 (s), 132.01 (s), 129.37 (s), 127.72 (s), 126.97 (s), 124.67 (s), 123.57 (s), 123.22 (s), 115.69 (s), 104.45 (s), 55.84 (s). ESI-TOF: $C_{32}H_{24}N_2OS$, m/z calcd for $[M+H]^+$ 485.16, found, 485.1691.

TZ-2 and **TZ-3** have been prepared and purified in the same conditions as **TZ-1** with yield of 80%, 75%, respectively.

TZ-2 ^{1}H NMR (400 MHz, DMSO) δ 8.11 (d, J = 8.5 Hz, 2H), 7.97 (d, J = 8.9 Hz, 1H), 7.85 (d, J = 8.5 Hz, 2H), 7.73 (dd, J = 13.3, 5.6 Hz, 3H), 7.36 (t, J = 7.9 Hz, 4H), 7.21-7.04 (m, 9H), 3.88 (s, 3H). ^{13}C NMR (101 MHz, $CDCl_3$) δ 167.86 (s), 154.12 (s), 148.00 (s), 147.52 (s), 143.22 (s), 134.84 (s), 133.52 (s), 131.89 (s), 129.24 (s), 128.18-127.67 (m), 127.00 (s), 126.38 (s), 125.17 (s), 124.71 (s), 123.53-123.05 (m), 121.63 (s). ESI-TOF: $C_{31}H_{22}N_2S$, m/z calcd for $[M+H]^+$ 455.15, found, 455.1588.

TZ-3: ^{1}H NMR (400 MHz, $CDCl_3$) δ 8.20-8.11 (m, 3H), 7.73 (d, J = 7.9 Hz, 2H), 7.60 (dd, J = 8.0, 2.4 Hz, 1H), 7.54 (d, J = 8.6 Hz, 2H), 7.29 (dd, J = 13.2, 5.7 Hz, 5H), 7.15 (d, J = 7.9 Hz, 6H), 7.07 (t, J = 7.3 Hz, 2H). ^{13}C NMR (101 MHz, $CDCl_3$) δ 167.71 (s), 161.74 (s), 159.30 (s), 150.53 (s), 148.01 (s), 147.48 (s), 143.40 (s), 135.85 (d, *J* = 11.2 Hz), (133.33, 131.42) (C-F, J=193.6 Hz) , 129.39 (s), 127.99 (s), 127.87 (d, *J* = 22.2 Hz), 127.05 (s), 124.74 (s), 123.97 (d, *J* = 9.3 Hz), 123.38 (d, *J* = 15.5 Hz), 115.21 (s), 114.96 (s), 108.04 (s), 107.77 (s). ESI-TOF: $C_{31}H_{21}FN_2S$, m/z calcd for $[M+H]^+$ 473.14, found, 473.1525.

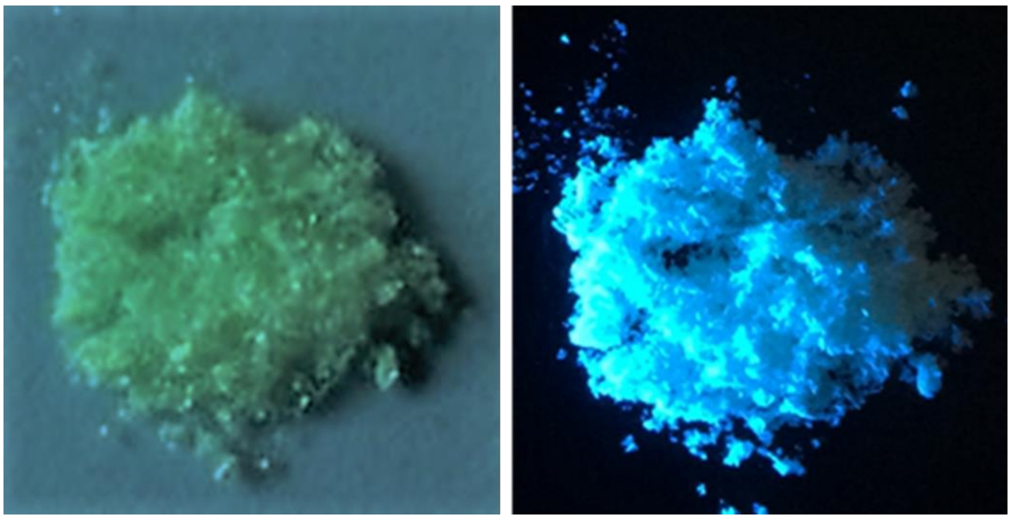

Figure S1. Image of original powder (**TZ-1**) under visible light (left) and UV light (right).

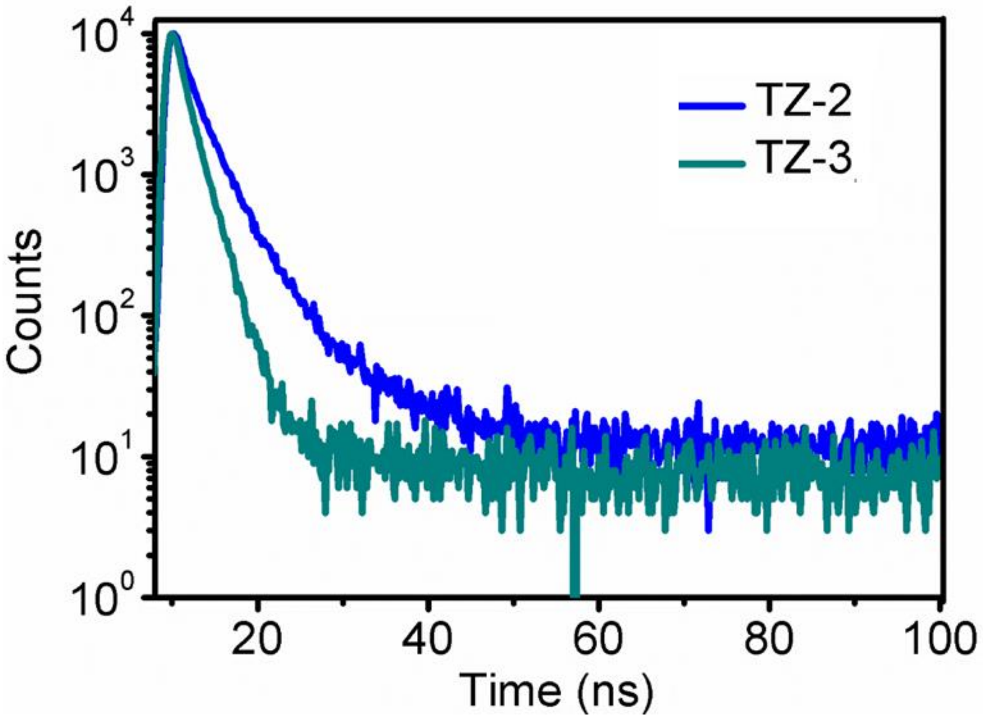

Figure S2. Transient decay spectra of **TZ-2**, and **TZ-3** crystals.

The fluorescence of crystals TZ-2 (blue line), TZ-3 (green line) all decay mono-exponentially with the time constant of 3.0 ns for TZ-2 crystals, 4.0 ns for TZ-3 crystals.

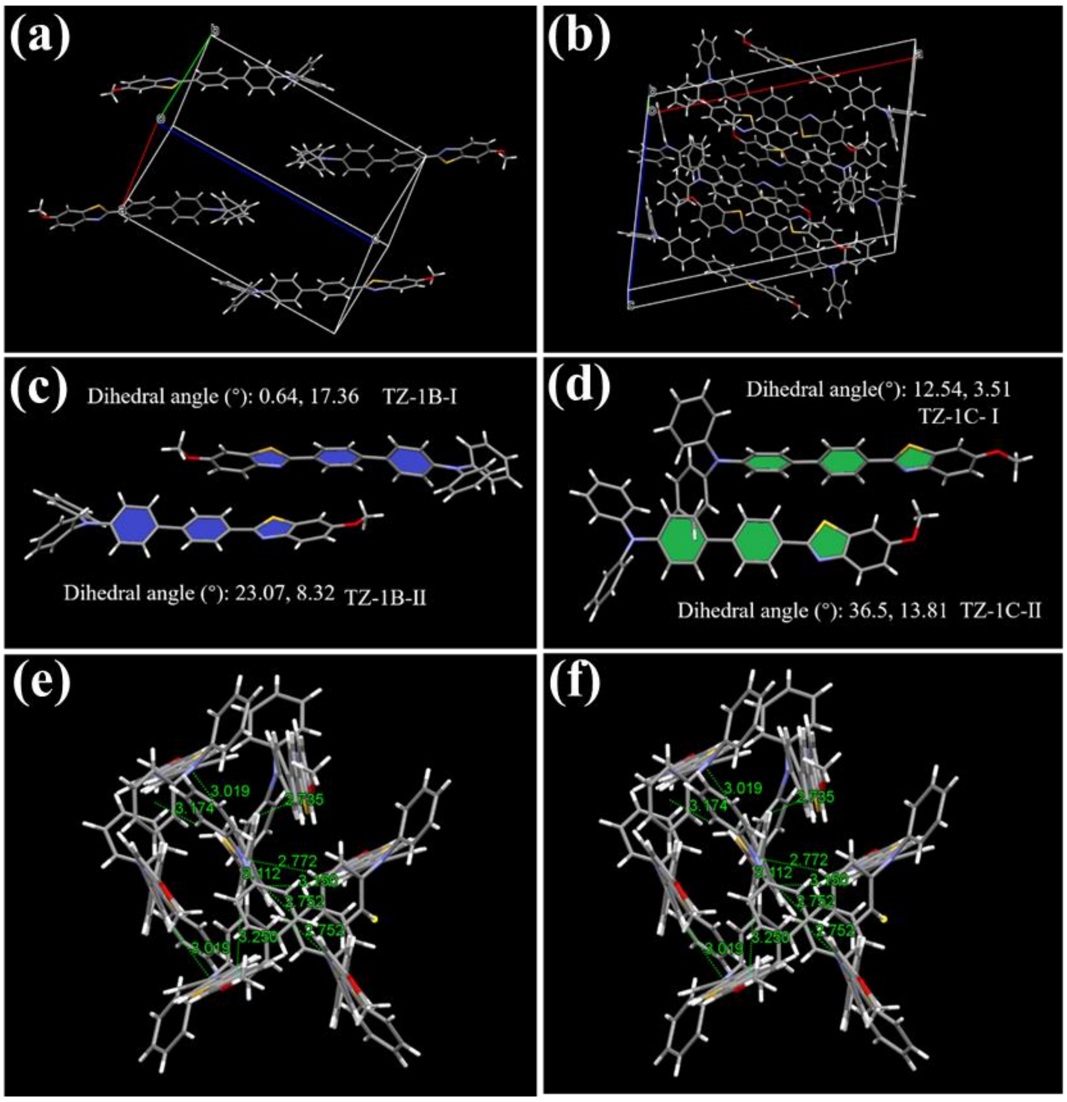

Figure S3. The unit cell, molecular conformations and intermolecular interactions of **TZ-1B** (a), (c), (e) and **TZ-1C** (b), (d), (f) with adjacent molecules.

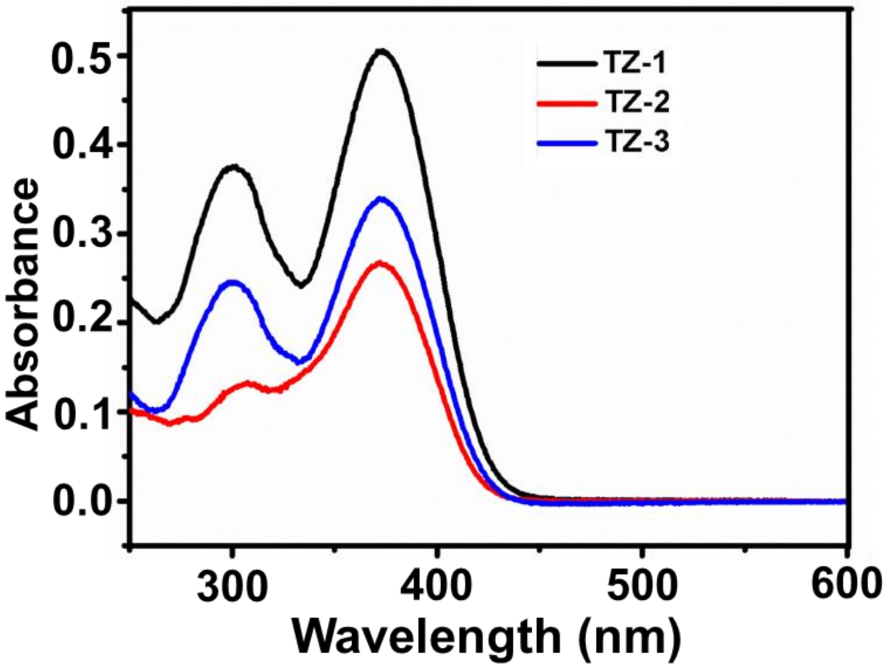

Figure S4. Absorption spectra of **TZ-1**, **TZ-2**, and **TZ-3** in DCM solution (1×10^{-5} M) at room temperature.

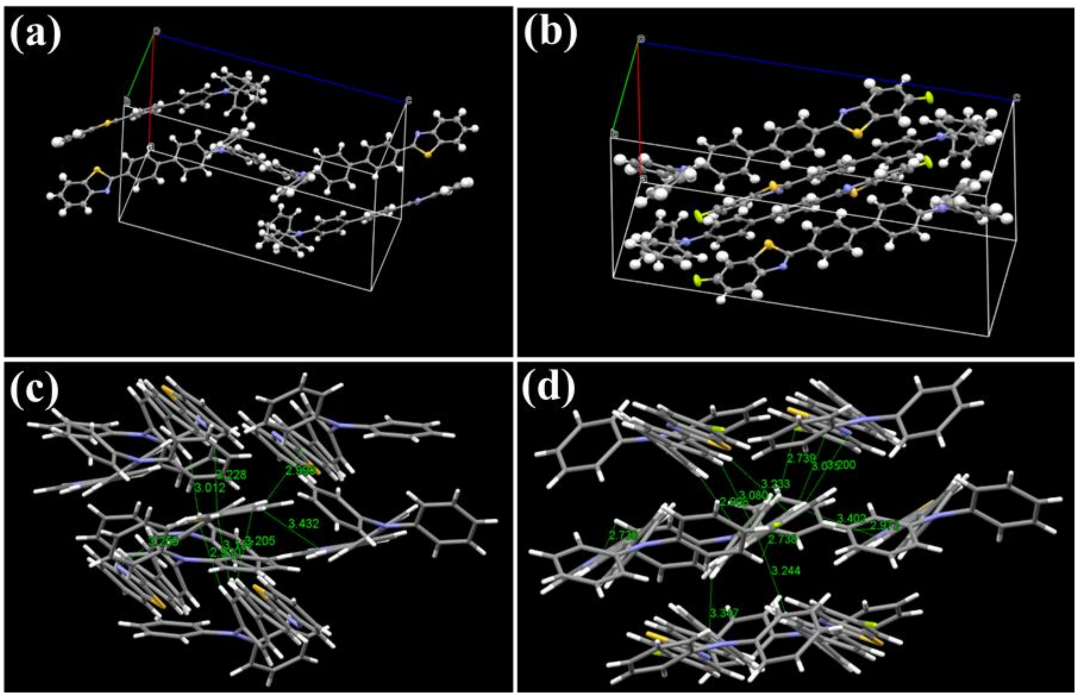

Figure S5. The unit cell, intermolecular interactions of **TZ-2** (a), (c), and **TZ- 3** (b), (d) with adjacent molecules.

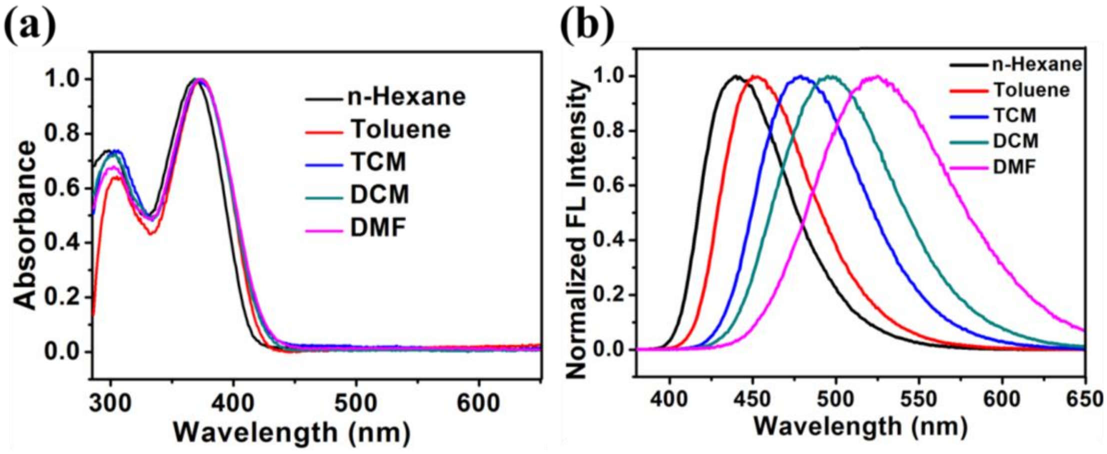

Figure S6. (a) UV absorption and (b) Emission (λ_{exc}=365 nm) spectra of **TZ-3** in different solvents (1×10^{-5} mol/L).

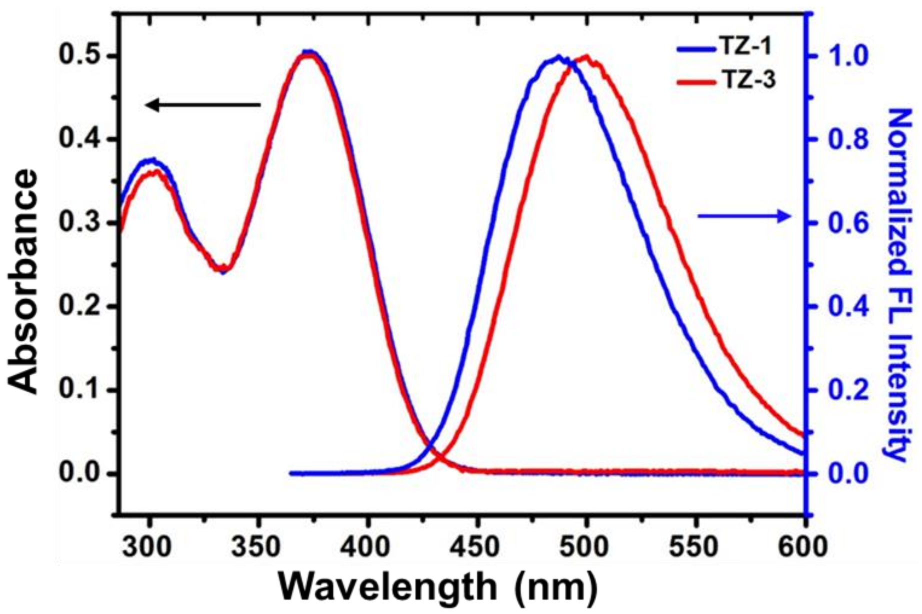

Figure S7. Absorption and Emission (λ_{exc}=365 nm) spectra of **TZ-1** and **TZ-3** in DCM solution (1×10^{-5} mol/L).

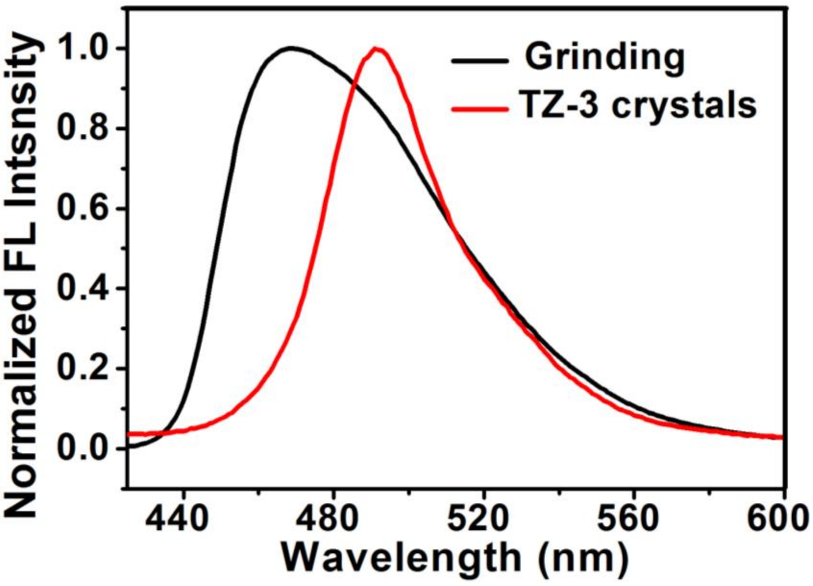

Figure S8. Normalized emission spectra (λ_{exc}=365 nm) of **TZ-3** crystals before (red line) and after ground (black line).

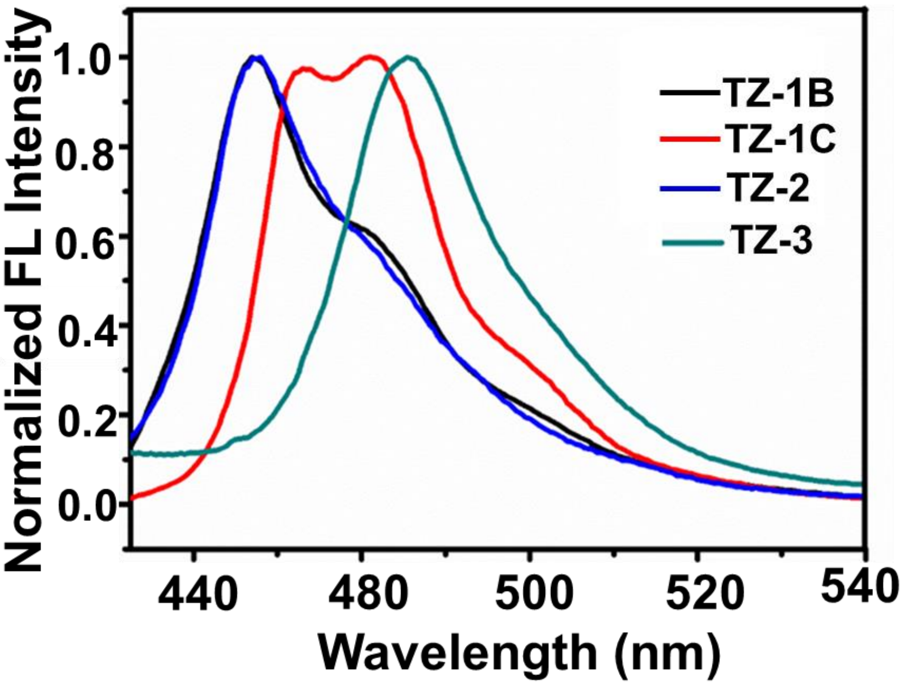

Figure S9. Emission spectra (λ_{exc}=365 nm) of **TZ-1B**, **TZ-1C**, **TZ-2**, and **TZ-3** crystals

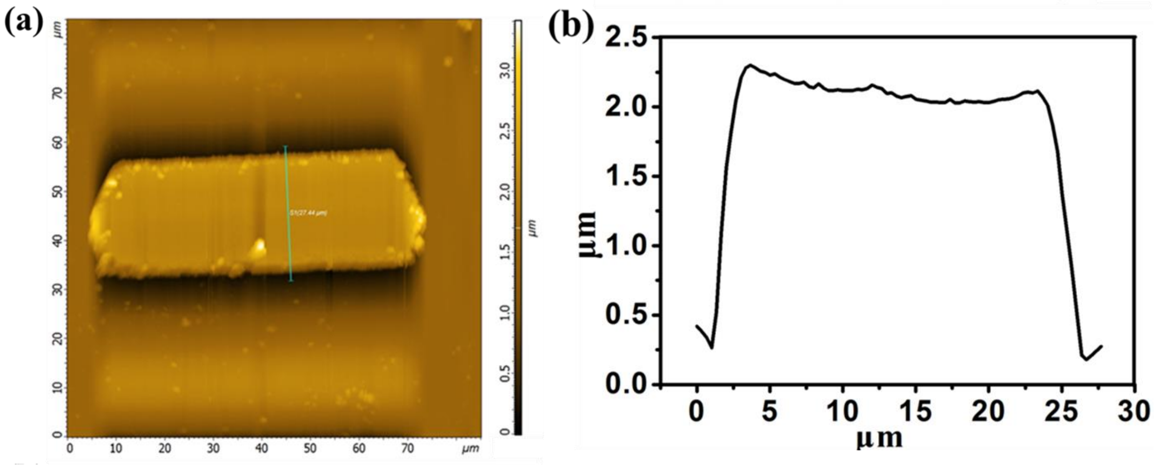

Figure S10. (a) Atomic force microscopic (AFM) image of **TZ-1B**; (b) Corresponding cross-sectional profile indicated in (a). The AFM image illustrates that **TZ-1B** has smooth surface and uniform height of about 2 μm.

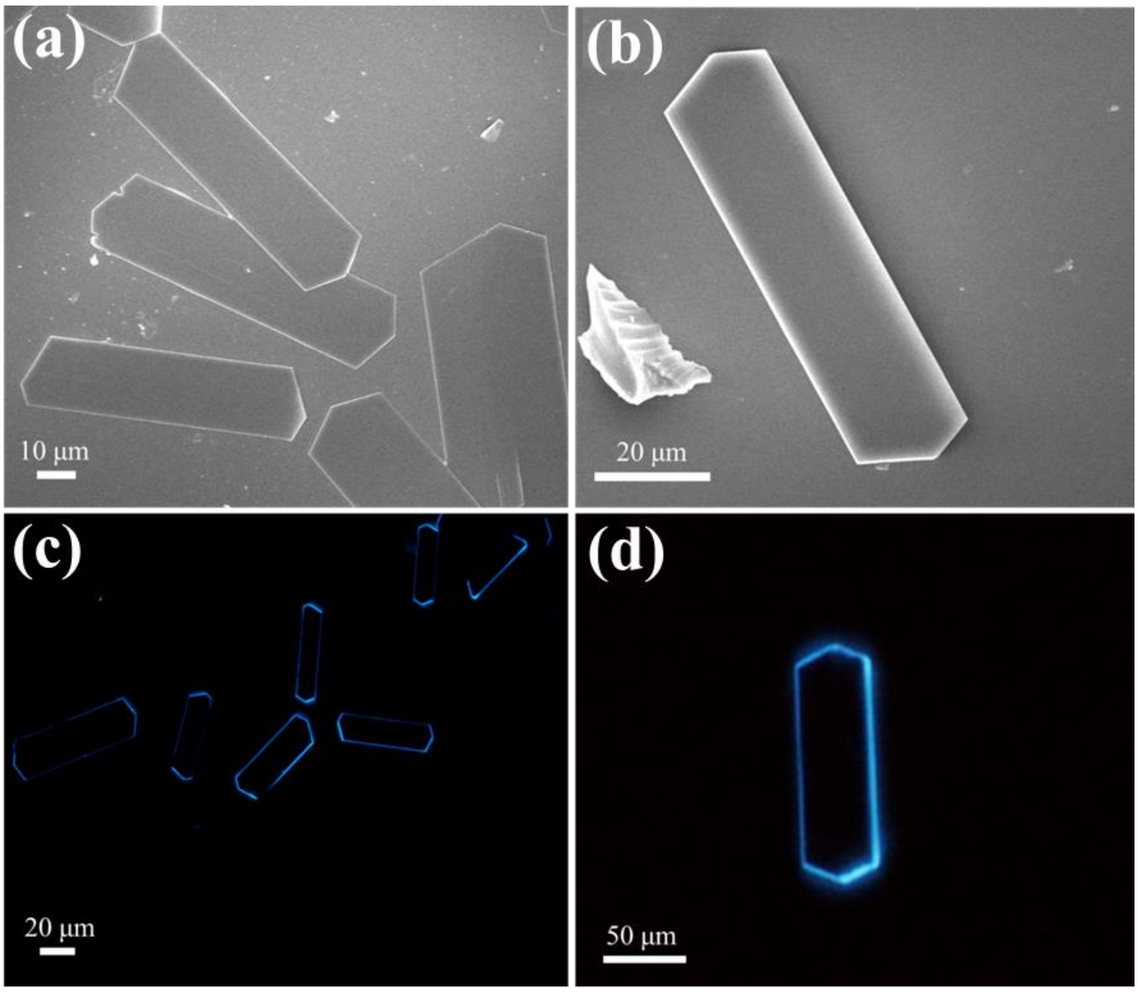

Figure S11. (a), (b) SEM and (c), (d) FL microscopy image of **TZ-1B** crystals excited with UV band of mercury lamp.

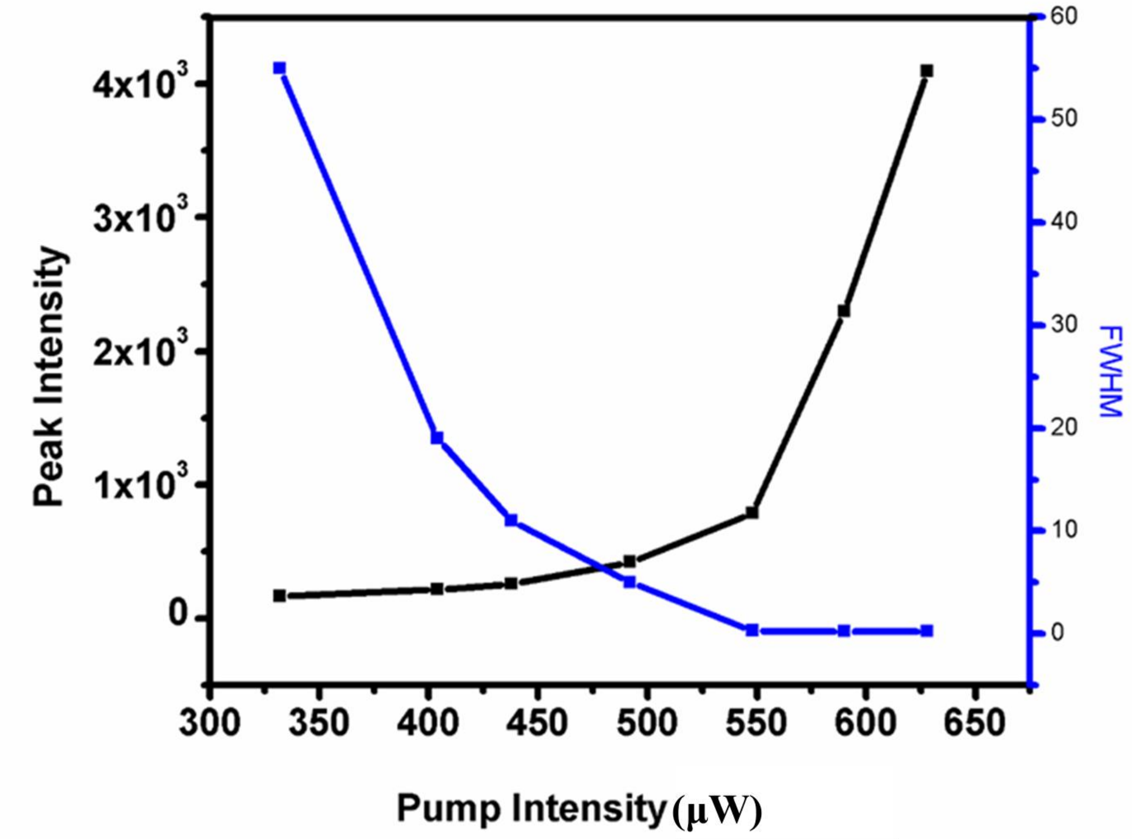

Figure S12. Power-dependent profiles of the FL peak intensity and FWHM of **TZ-1B**.

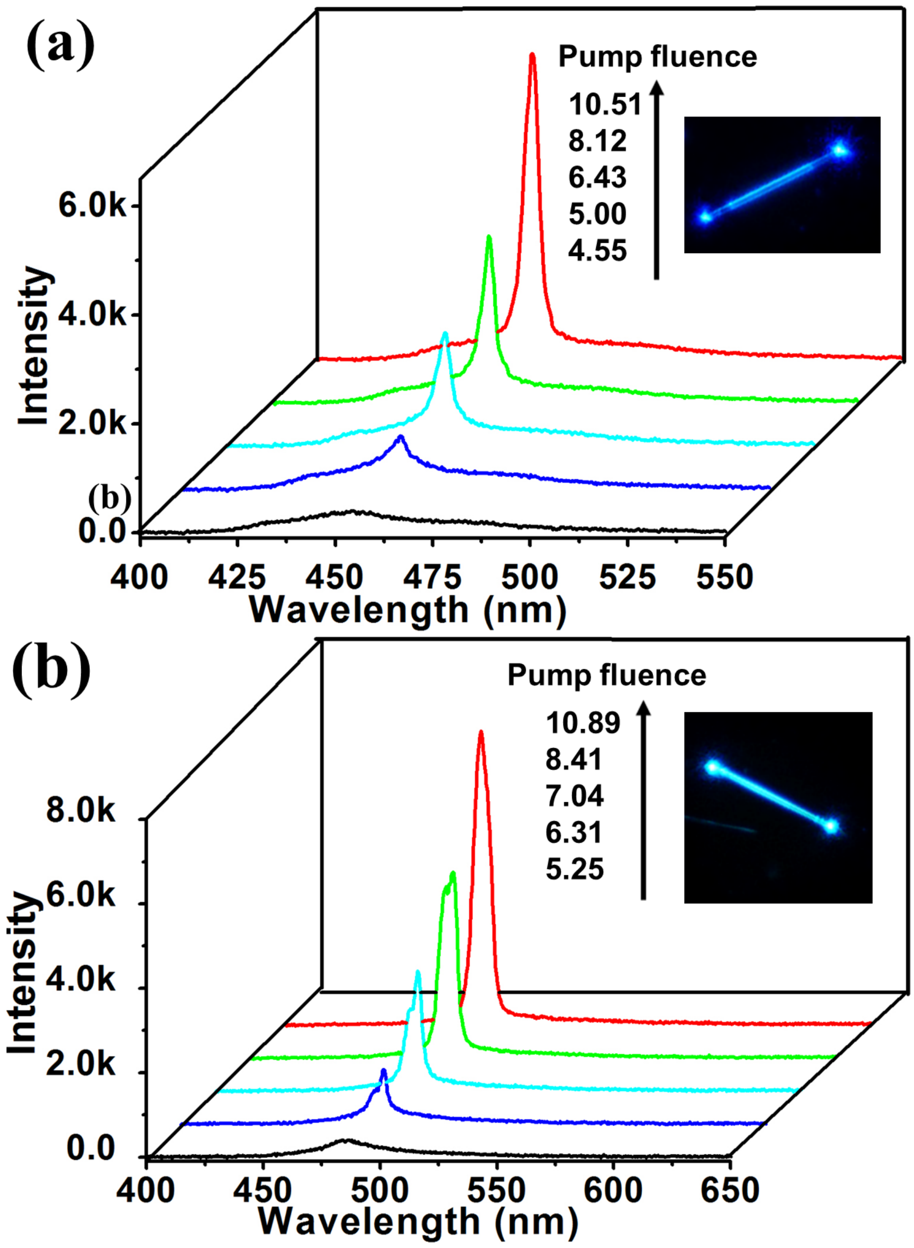

Figure S13. FL spectra of individual **TZ-2** (a) and **TZ-3** (b) at different laser pump fluence. Inset: Optical images of **TZ-2** and **TZ-3** above lasing threshold.

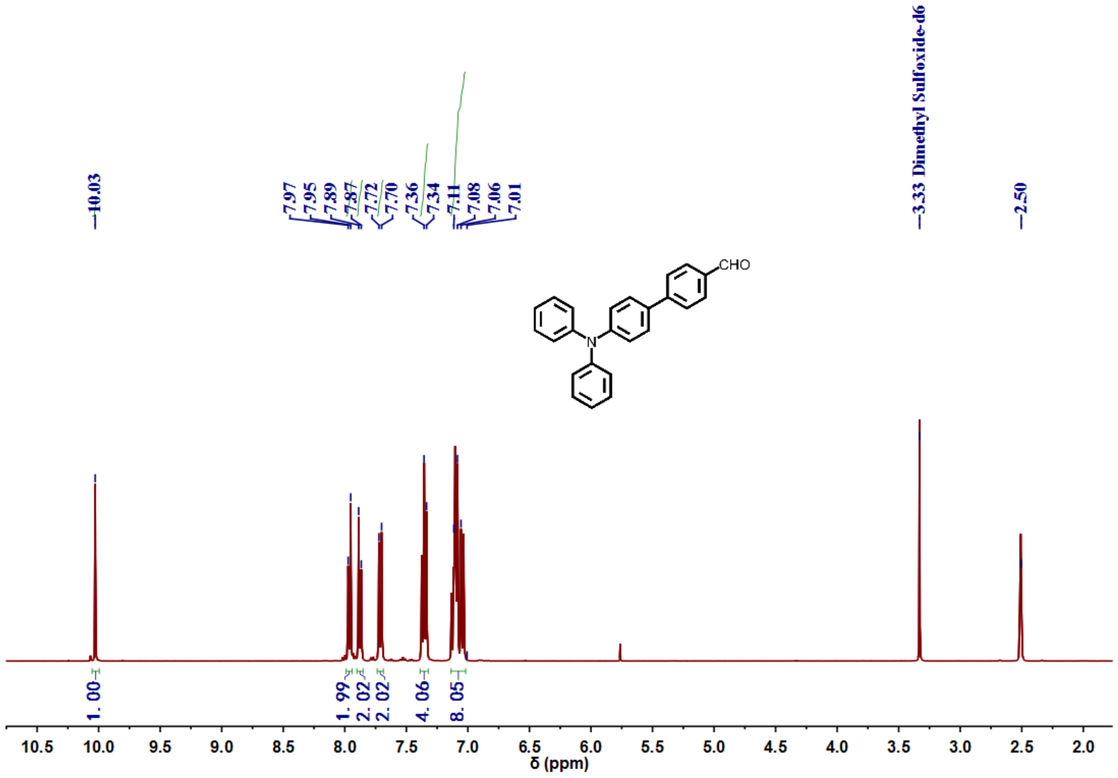

Figure S14. ^{1}H-NMR spectrum of **TPA-CHO** in DMSO.

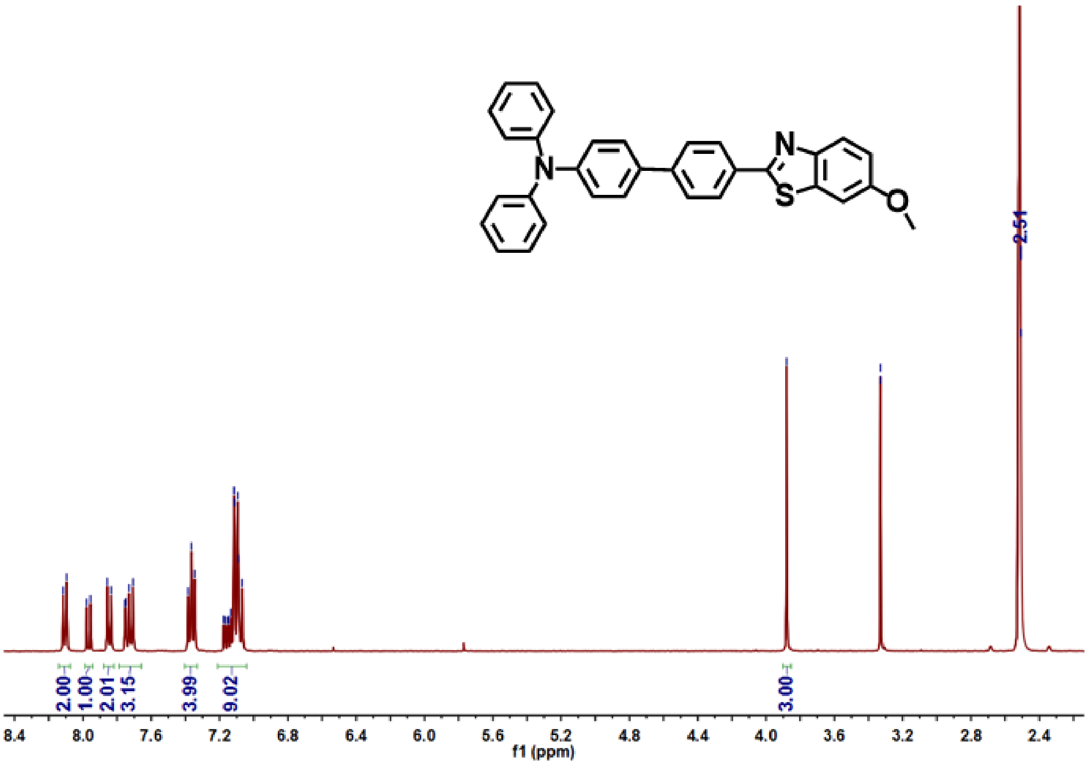

Figure S15. ^{1}H-NMR spectrum of **TZ-1** in DMSO.

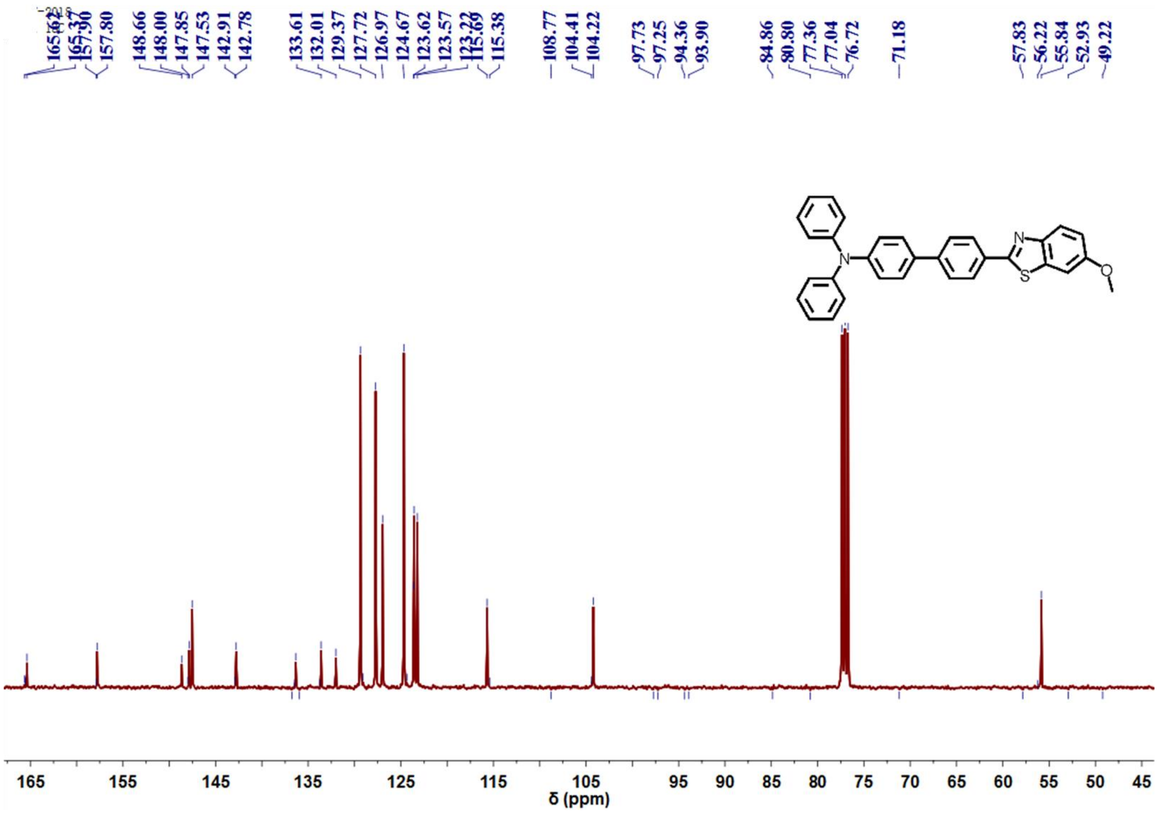

Figure S16. ^{13}C-NMR spectrum of **TZ-1** in $CDCl_3$.

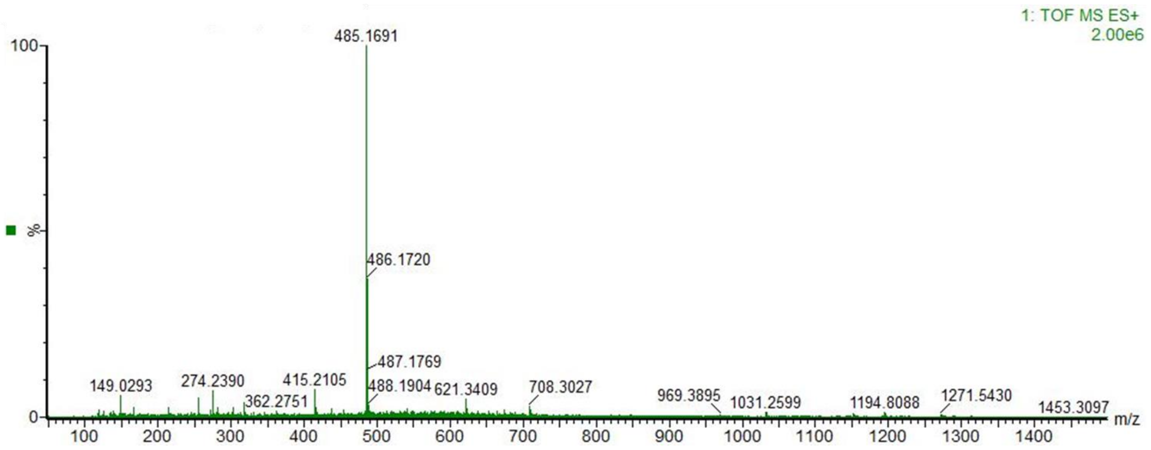

Figure S17. ESI-TOF of **TZ-1**.

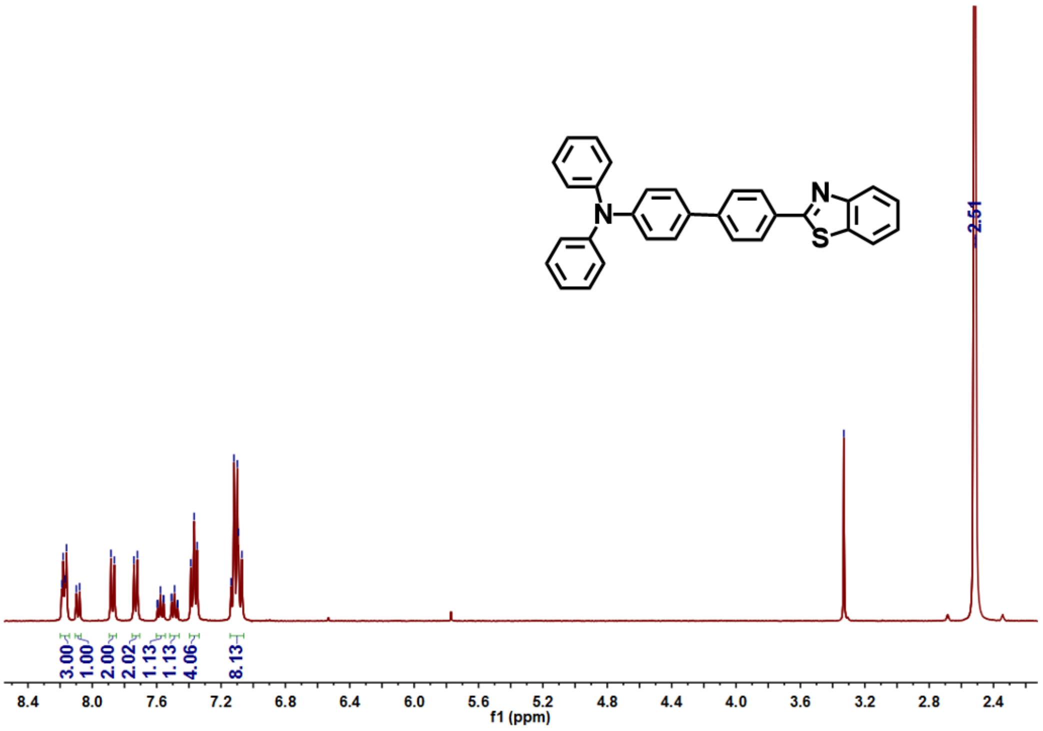

Figure S18. ^{1}H-NMR spectrum of **TZ-2** in DMSO.

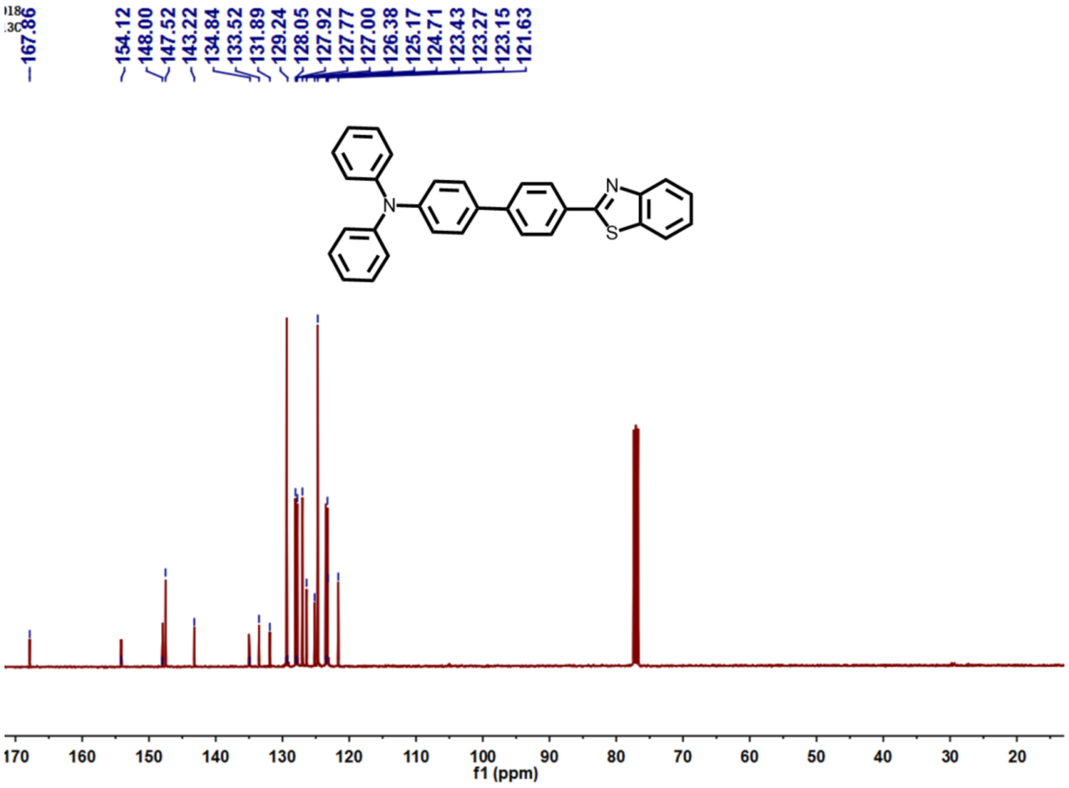

Figure S19. ^{13}C-NMR spectrum of **TZ-2** in $CDCl_3$.

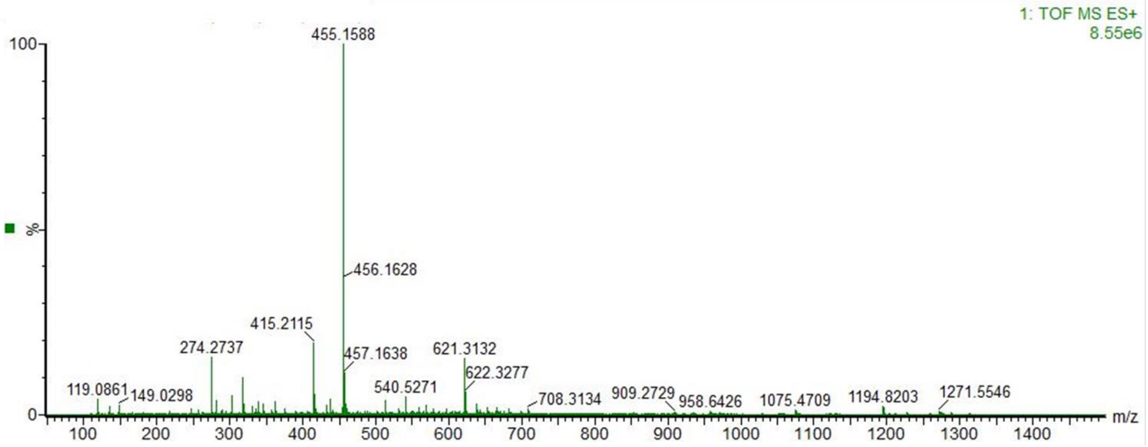

Figure S20. ESI-TOF of **TZ-2**.

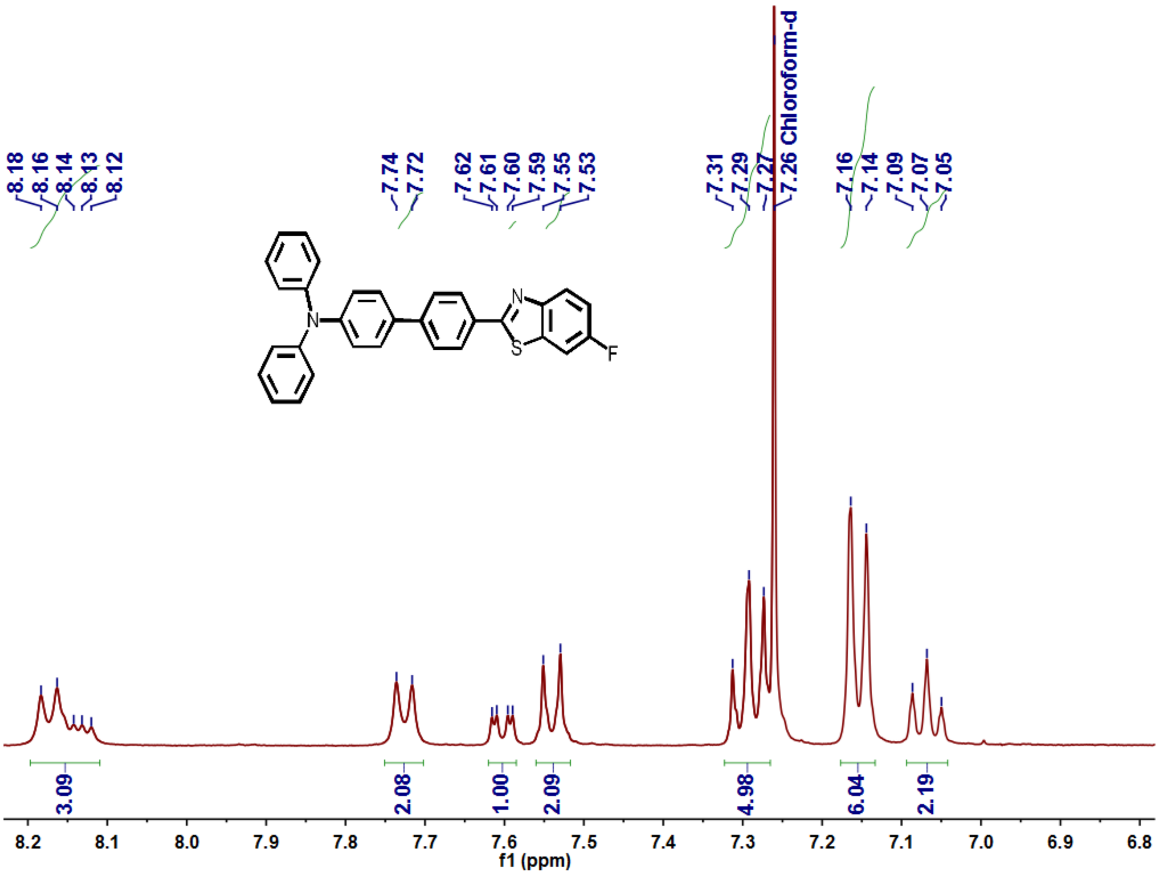

Figure S21. ^{1}H-NMR spectrum of **TZ-3** in $CDCl_3$.

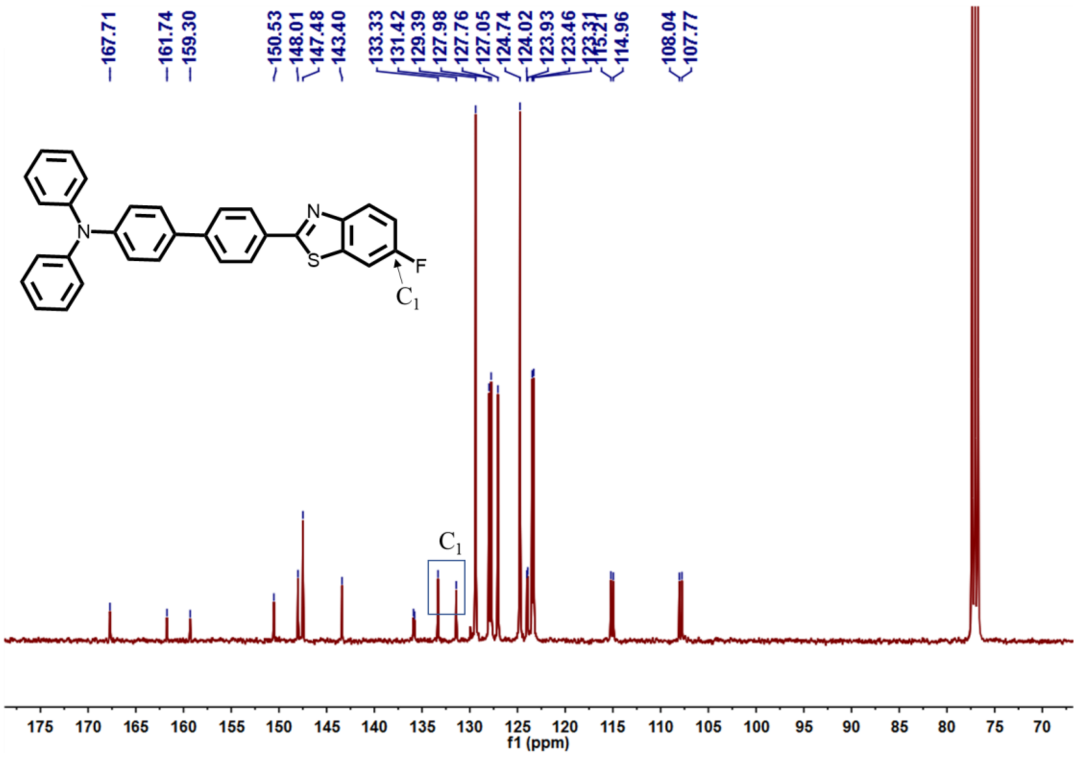

Figure S22. ^{13}C-NMR spectrum of **TZ-3** in CDCl$_3$.

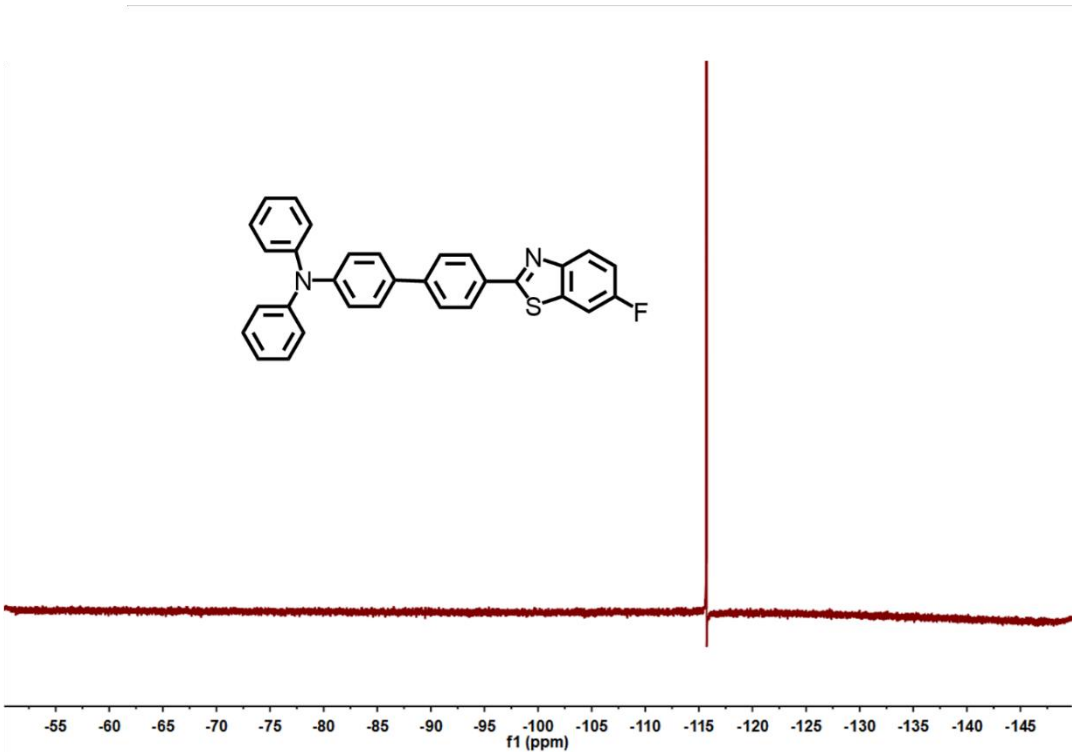

Figure S23. ^{19}F-NMR spectrum of **TZ-3** in DMSO.

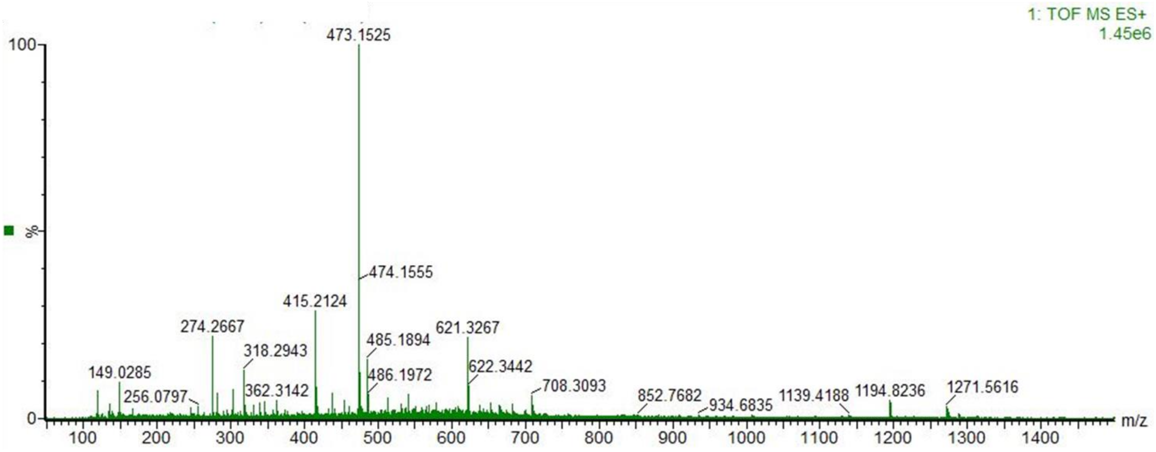

Figure S24. ESI-TOF of **TZ-3**.

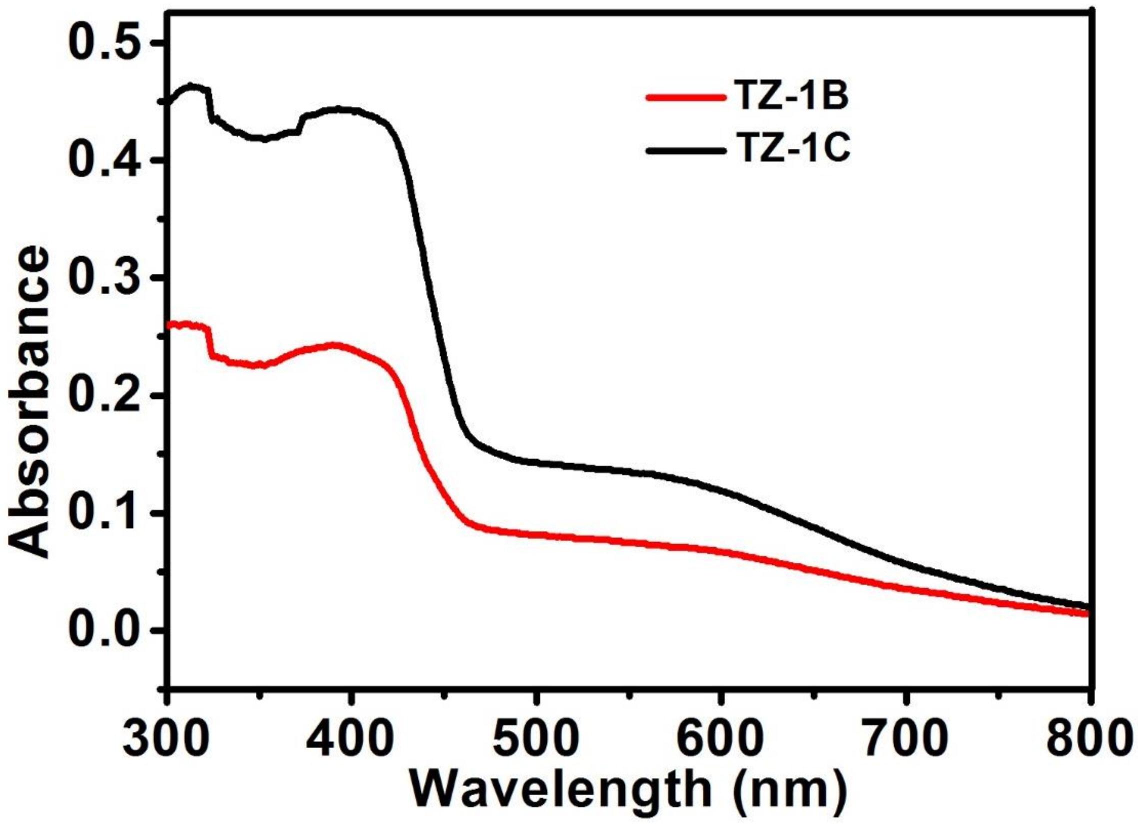

Figure S25. Whole absorption spectra of **TZ-1B** and **TZ-1C** monocrystals.

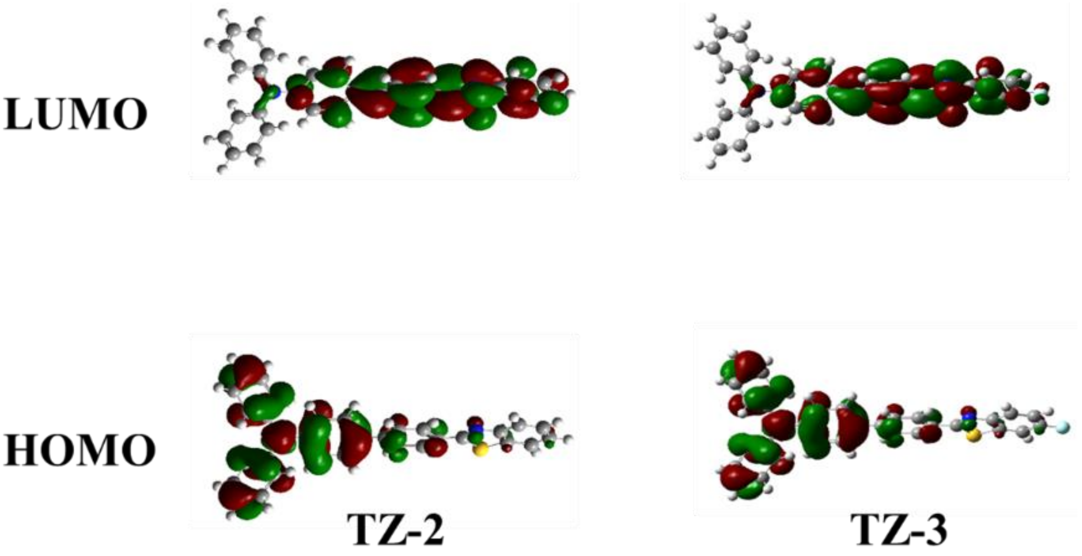

Figure S26. The frontier orbital plots of HOMO and LUMO of TZ-2 and TZ-3.

Table S1. Crystal data and structure refinement for **TZ-1B**, **TZ-1C**, **TZ-2** and **TZ-3**.

Identification code	**TZ-1B**	**TZ-1C**	**TZ-2**	**TZ-3**
Empirical formula	$C_{32}H_{24}N_2OS$	$C_{32}H_{24}N_2OS$	$C_{31}H_{22}N_2S$	$C_{31}H_{21}FN_2S$
Formula weight	484.59	484.59	454.57	472.56
Crystal system	triclinic	monoclinic	triclinic	triclinic
Space group	P-1	P21/c	P-1	P-1
a / Å,	10.1910(8)	27.6059(14)	10.1133(5)	10.1027(8)
b / Å	11.321(2)	9.1497(5)	10.3101(4)	10.4117(9)
c / Å	23.832(4)	20.3003(7)	23.8885(10)	23.9864(17)
α/°	99.689(16)	90.00	82.681(4)	84.600(3)
β/°	94.889(11)	108.196(5)	82.685(4)	82.776(2)
γ/°	115.002(13)	90.00	66.954(4)	66.337(3)
Volume ($Å^3$)	2418.5(7)	4871.2(4)	2265.17(17)	2289.9(3)
Z	4	8	4	4